TISSUE ENGINEERING: Part A
Volume 18, Numbers 15 and 16, 2012

DOI: 10.1089/ten.tea.2011.0604

Biofunctionalized Calcium Phosphate Cement to Enhance the Attachment and Osteodifferentiation of Stem Cells Released from Fast-Degradable Alginate-Fibrin Microbeads

Hongzhi Zhou, D.D.S., Ph.D.,[1,2] Wenchuan Chen, D.D.S., Ph.D.,[1]
Michael D. Weir, Ph.D.,[1] and Hockin H.K. Xu, Ph.D.[1,3–5]

Stem cell-encapsulating microbeads could be mixed into a paste such as calcium phosphate cement (CPC), where the microbeads could protect the cells from the mixing and injection forces. After being placed, the microbeads could quickly degrade to release the cells throughout the scaffold, while creating macropores. The objectives of this study were to (1) construct alginate-fibrin microbeads encapsulating human umbilical cord mesenchymal stem cells (hUCMSCs) embedded in the surface of novel biofunctionalized CPC and (2) investigate microbead degradation, cell release, and osteodifferentiation on CPC. Hydrogel microbeads were fabricated that encapsulated hUCMSCs at 1×10^6 cells/mL. CPC was biofunctionalized with fibronectin (Fn) and Arg-Gly-Asp (RGD). Four scaffolds were tested: CPC control, CPC mixed with Fn, CPC mixed with RGD, and CPC grafted with RGD. The degradable microbeads released hUCMSCs at 7 days, which attached to CPC. Adding Fn or RGD to CPC greatly improved cell attachment. CPC grafted with RGD showed the fastest cell proliferation, with cell density being ninefold that on CPC control. The released hUCMSCs underwent osteodifferentiation. Alkaline phosphatase, osteocalcin, collagen 1, and runt-related transcription factor 2 (Runx2) gene expression increased by 10 to 30 fold at 7–21 days, compared with day 1. The released cells on CPC synthesized bone minerals, with the mineralization amount at 21 days being two orders of magnitude higher than that at 7 days. In conclusion, alginate-fibrin microbeads embedded in CPC surface were able to quickly release the hUCMSCs that attached to biofunctionalized CPC. Incorporating Fn and RGD into CPC greatly improved cell function, and CPC grafted with RGD had the fastest cell proliferation. The released cells on CPC differentiated into the osteogenic lineage and synthesized bone minerals. The new biofunctionalized CPC with hUCMSC-encapsulating microbeads is promising for bone regeneration applications.

Introduction

Tissue engineering employs stem cells and scaffolds to repair and regenerate the lost or diseased tissues.[1–4] Bone tissue engineering grew out of the increasing need for bone repair due to skeletal diseases, congenital malformations, trauma, and tumor resections.[5–9] Extensive studies have been performed on stem cells and novel scaffolds for osteogenic differentiation and bone regeneration.[10–13] Alginate hydrogels were used as scaffolds because they could be cross-linked under mild conditions without damage to the cells, and they were highly hydrated with good biocompatibility.[14,15] Another class of scaffolds consisted of calcium phosphate cements (CPCs).[16–18] One such cement consisted of tetracalcium phosphate and dicalcium phosphate anhydrous and was referred to as CPC. CPC had excellent osteoconductivity, was bioresorbable, and could be replaced by new bone.[19,20] Previous studies incorporated chitosan (CN) and absorbable fibers to increase the load-bearing capability of CPC.[21,22] In recent studies,[23,24] cells were encapsulated in alginate microbeads, and the microbeads were mixed into CPC, which served as a moderate load-bearing scaffold for cell delivery.[23]

Recently, stem-cell-encapsulating alginate microbeads with sizes of several hundred micrometers were fabricated, which were suitable for injection delivery.[23] These microbeads were mixed into the CPC paste, and the paste could be injected and then set to form a scaffold without compromising

[1]Biomaterials & Tissue Engineering Division, Department of Endodontics, Prosthodontics and Operative Dentistry, University of Maryland School of Dentistry, Baltimore, Maryland.
[2]Department of Oral & Maxillofacial Surgery, School of Stomatology, Fourth Military Medical University, Xi'an, China.
[3]Center for Stem Cell Biology & Regenerative Medicine and [4]Marlene and Stewart Greenebaum Cancer Center, University of Maryland School of Medicine, Baltimore, Maryland.
[5]Department of Mechanical Engineering, University of Maryland, Baltimore County, Maryland.

the cell viability and function.[23] The alginate microbeads protected the cells from the mixing and injection forces as well as the CPC setting reaction.[23] After the CPC has set, it is desirable for the microbeads to degrade quickly in order to release the cells throughout the CPC scaffold, while concomitantly creating macropores in CPC. However, the alginate microbeads in these previous studies did not degrade quickly.[23] Since the initial setting reaction of CPC takes only several minutes, and complete setting takes about a day, it is desirable for the microbeads to degrade in a few days to release the cells to enhance cell function. Partially oxidized alginate scaffolds degraded hydrolytically in several weeks to a few months.[25] A recent study showed that adding a small amount of fibrin dramatically increased the degradation rate for the alginate microbeads.[26] The novel alginate-fibrin microbeads with sizes of several hundred micrometers quickly degraded and released the cells in only several days.[26]

In the previous study,[26] the microbeads were placed in the tissue culture polystyrene (TCPS) wells without CPC. The eventual goal is to mix the microbeads into CPC paste and to investigate cell release and attachment inside the CPC scaffold. However, once the CPC construct is fractured and opened for examination, it would be difficult to image cell attachment and viability on the tortuous and rough fracture surfaces of CPC. Therefore, in the present study, the surface of a fleshly mixed CPC paste was rendered flat, and then the cell-encapsulating microbeads were placed on the CPC paste and lightly pressed to be partially embedded into the CPC paste. After CPC setting, the microbeads were locked in the CPC surface. In the culture media, the microbeads gradually degraded and released the cells, which attached to the flat CPC surface, allowing live/dead staining and microscopic examination.

Hence, the objective of this study was to investigate stem cell release from fast-degradable microbeads with attachment and osteogenic differentiation on CPC. It was hypothesized that (1) oxidized alginate-fibrin microbeads embedded in the CPC surface will quickly release the stem cells to attach to the CPC surface, (2) the released stem cells on CPC can differentiate into the osteogenic lineage and synthesize bone minerals *in vitro*, and (3) the proliferation and osteogenic differentiation of the released stem cells will be greatly improved via incorporation of biofunctional agents in CPC.

Materials and Methods

Human umbilical cord mesenchymal stem cell culture

The use of human umbilical cord mesenchymal stem cells (hUCMSCs) (ScienCell, Carlsbad, CA) was approved by the University of Maryland. Cells were harvested from the Wharton's Jelly in umbilical cords of healthy babies, using a procedure described previously.[27] Cells were cultured in a low-glucose Dulbecco's modified Eagle's medium with 10% fetal bovine serum and 1% penicillin–streptomycin (Invitrogen, Carlsbad, CA) (control media). hUCMSCs at 80%–90% confluence were detached and passaged. Passage 4 cells were used in this study. The osteogenic media consisted of the control media plus 100 nM dexamethasone, 10 mM β-glycerophosphate, 0.05 mM ascorbic acid, and 10 nM 1α,25-Dihydroxyvitamin (Sigma, St. Louis, MO).[28]

Synthesis of hydrogel microbeads with hUCMSC encapsulation

Alginate is noncytotoxic and can form an ionically cross-linked network under mild conditions without damaging the encapsulated cells.[23,26] Alginate was oxidized to increase its degradability. Oxidation was done using sodium periodate at the correct stoichiometric ratio of sodium periodate/alginate to have certain percentages of alginate oxidation.[25] The percentage of oxidation (%) was the number of oxidized uronate residues per 100 uronate units in the alginate chain.[25] In the present study, alginate at 7.5% oxidation was synthesized. The alginate oxidation followed previous procedures.[25] Briefly, 1% by mass of sodium alginate (ProNova, Oslo, Norway) was dissolved in distilled water. About 1.51 mL of 0.25 M sodium periodate (Sigma) was added to 100 mL of alginate solution, which was stirred to react in the dark at room temperature. At 24 h, the oxidization reaction was stopped by adding 1 g of ethylene glycol and then 2.5 g of sodium chloride. Ethanol of 200 mL was added to precipitate the product. The precipitates were re-dissolved in 100 mL of water and precipitated with 200 mL of ethanol. The final product was freeze dried for 24 h, and used to make the microbeads.

The oxidized alginate was dissolved in saline at a concentration of 1.2%.[26] Fibrinogen from bovine plasma (Sigma) was added at a concentration of 0.1% to the alginate solution. hUCMSCs were added to the alginate-fibrinogen solution at a density of 1×10^6 cells/mL. The alginate–cell solution was loaded into a syringe that was connected to a bead-generating device (Var J1; Nisco, Zurich, Switzerland). Nitrogen gas was fed to the gas inlet and a pressure of 8 psi was established to form a coaxial air flow to break up the alginate droplets. To cross-link the microbeads, a solution containing 125 mL of 100 mM calcium chloride plus 125 NIH units of thrombin (Sigma) was prepared. When the alginate-fibrinogen droplets were sprayed into this solution, calcium chloride caused the alginate to cross-link, while the reaction between fibrinogen and thrombin produced fibrin. This yielded hUCMSC-encapsulating, oxidized alginate-fibrin microbeads. The entire process from preparing the cell-alginate solution to the microbead collection took ~30 min. Preliminary live/dead assay showed nearly 100% live cells and few dead cells in the microbeads. A recent study showed that the alginate-fibrin microbeads were slightly elongated in shape.[26] The measurement of 100 microbeads showed a length range of 87–580 μm (mean = 335 μm), and the width range of 75–345 μm (mean = 232 μm).[26] These oxidized alginate-fibrin microbeads are referred to as "microbeads."

hUCMSC-encapsulating microbeads in CPC surface

The hydrogel microbeads could protect the encapsulated cells from the CPC paste mixing forces and the setting reaction. After CPC had set, the purpose was for the microbeads to quickly degrade and release the cells. To examine this approach, the alginate-fibrin microbeads with hUCMSC encapsulation were seeded into the surface layer of the CPC paste.

The CPC powder consisted of a mixture of tetracalcium phosphate (TTCP), $Ca_4(PO_4)_2O$, and dicalcium phosphate anhydrous (DCPA), $CaHPO_4$. TTCP was synthesized from a

solid state reaction between $CaHPO_4$ and $CaCO_3$ (Baker Chemical, Phillipsburg, NJ) in a furnace at 1500°C for 6 h. The TTCP was then ground and sieved to obtain particles with sizes ranging from about 1 to 60 μm, with a median size of 17 μm. DCPA was obtained commercially (Baker Chemical) and grounded to obtain particles of 0.4 to 3.0 μm, with a median of 1.0 μm. TTCP and DCPA were mixed at 1:3 molar ratio to form the CPC powder. Type I bovine collagen fiber (Sigma) was added to CPC at a mass fraction of 5%. CPC liquid consisted of CN lactate (Vanson, Redmond, WA) dissolved in water at a CN/(CN+water) mass fraction of 15%.[21] CN and its derivatives are natural biopolymers that are biodegradable and osteoconductive,[29] and can impart fast-setting and high strength to CPC.[30] A CPC powder:liquid mass ratio of 2:1 was used to form a flowable paste.[23] The CPC paste was filled into a disk mold of 15-mm diameter and 2-mm height, and the paste surface was flattened with a glass slide. Then, 0.2 mL of hUCMSC-encapsulating microbeads was placed on the CPC paste and gently pressed to be partially embedded into the paste. After incubating for 10 min in a humidor at 37°C and 100% humidity, the construct was transferred into a six-well plate. Five microliters of osteogenic media was added into each well. The microbead–CPC construct is schematically shown in Figure 1A.

Development of novel biofunctionalized CPC

Preliminary study indicated that after hUCMSCs were released from the microbeads, cell attachment to CPC was relatively poor. Therefore, biofunctional molecules were incorporated into CPC to improve cell attachment. Four groups were tested: CPC control (no biofunctional agents), CPC mixed with fibronectin (Fn), CPC mixed with RGD, and CPC grafted with RGD.

Fn from bovine plasma (Sigma) was mixed with the CN liquid, which was then mixed with CPC powder. Fn was shown to improve cell attachment to scaffolds.[31,32] Based on our preliminary study, 0.25 mg of Fn was mixed in each CPC disk, which greatly enhanced cell function. A CPC disk used 1 g of CPC paste; hence, the Fn concentration in CPC was 0.025% by mass. This biofunctionalized CPC is referred to as "CPC-mixed-Fn."

The tripeptide Arg-Gly-Asp (RGD) is an important functional and cell-binding domain.[2,4,32–34] RGD (Sigma) was

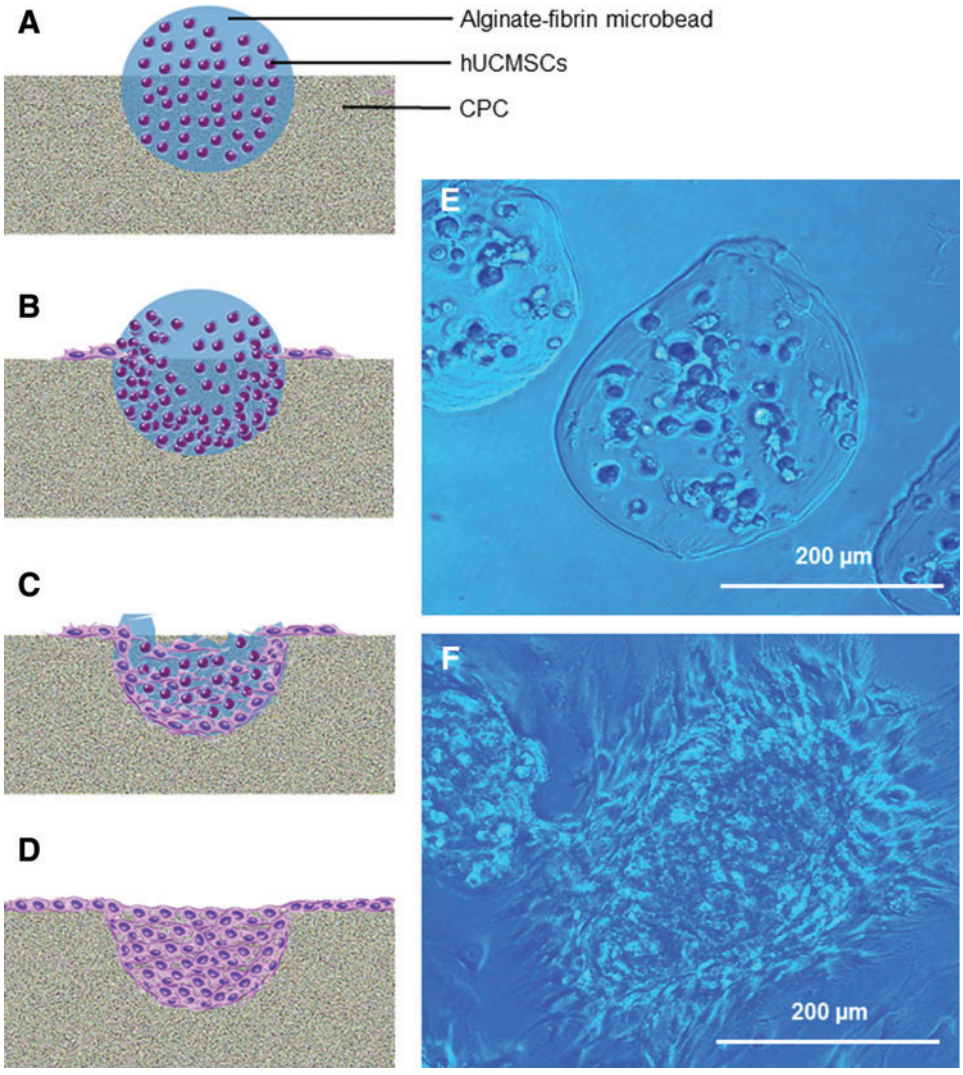

FIG. 1. Human umbilical cord mesenchymal stem cell (hUCMSC)–encapsulating alginate-fibrin microbeads embedded partially into biofunctionalized calcium phosphate cement (CPC) surface. **(A–D)** Schematic illustrating microbeads in CPC with cell release at 1, 7, 14, and 21 days, respectively. **(E, F)** Optical photos of microbeads at 1 and 14 days, respectively. A blue filter was used to enhance the contrast and clarity of microbeads. At day 1, there was no microbead degradation, and the encapsulated cells appeared as rounded dots. At 14 days, the microbeads degraded and the hUCMSCs were released, showing cell attachment with elongated and spreading morphology. Color images available online at www.liebertonline.com/tea

mixed with the CN liquid, which was then mixed with CPC. As for Fn, 0.25 mg of RGD was mixed into each CPC disk, yielding an RGD concentration of 0.025% by mass. This biofunctionalized CPC is referred to as "CPC-mixed-RGD."

For RGD grafting, oligopeptides with a sequence of (glycine)4-arginine-glycine-aspartic acid-serine-proline (abbreviated as G4RGDSP) (Peptides International, Louisville, KY) were covalently conjugated to CN and then mixed with CPC. 1-Ethyl-3-(3-dimethylaminopropyl) carbodiimide (EDC) in combination with sulfo-N-hydroxysuccinimide (NHS) were used as carboxyl-activating agents for the coupling of primary amines to yield amide bonds. Because EDC is a zero-length cross-linker, polypeptide like G4RGDSP with RGD as the functional sequence is frequently used as cell adhesion peptides for bioscaffold grafting by carbodiimide chemistry.[2,4,35] Briefly, CN was dissolved in 0.1 M MES buffer (Sigma) at 1%. EDC (Sigma), Sulfo-NHS (Sigma), and G4RGDSP peptide were added to CN at a molar ratio of G4RGDSP/EDC/NHS = 1/1.2/0.6, and allowed to react for 24 h. The products were dialyzed against water using a cellulose membrane (MWCO = 25 kDa) for 3 days and then freeze dried. This resulted in the RGD-grafted CN, which was dissolved in water at 15% to obtain the CN liquid. This RGD-grafted CN liquid was mixed with CPC powder. The same RGD concentration of 0.025% was used in CPC, taking into account that the molecular weight (MW) of G4RGDSP is 759, and the MW of RGD is 346. This biofunctionalized CPC is referred to as "CPC-grafted-RGD." It should be noted that RGD was grafted to the liquid portion (the CN) of CPC. RGD was not grafted to the powder portion of CPC.

Live/dead assay of hUCMSCs from microbeads and attachment on biofunctionalized CPC

The hUCMSC-encapsulating microbeads were embedded into the surface of the four different types of CPC pastes. The time periods for examination were 1, 7, 14, and 21 days, as schematically shown in Figure 1A–D. For the live/dead staining, each sample was incubated at 37°C for 10 min with 2 mL Tyrode's HEPES containing 2 μM calcein-AM and 2 μM ethidium homodimer-1 (Molecular Probes, Eugene, OR).[23] An epifluorescence microscopy (Nikon, Melville, NY) was used to examine the samples. Three random fields of view were imaged from each sample (six samples yielded 18 photos for each time point). The percentage of live cells was $P_L = N_L/(N_L + N_D)$, where N_L = the number of live cells and N_D = the number of dead cells. Live cell density was $D_L = N_L/A$, where A is the area of the view field for N_L.

Osteogenic differentiation of released cells on biofunctionalized CPC

The earlier experiments showed that CPC-grafted-RGD had the best cell attachment and proliferation. Hence, CPC-grafted-RGD was selected for osteogenic differentiation experiments. Quantitative real-time reverse transcription–polymerase chain reaction (qRT-PCR, 7900HT; Applied Biosystems, Foster City, CA) was used. Constructs were cultured for 1, 4, 7, 14, and 21 days in osteogenic media. The total cellular RNA of the cells was extracted with TRIzol reagent (Invitrogen) and reverse-transcribed into cDNA. TaqMan gene expression assay kits were used to measure the transcript levels of the proposed genes on human alkaline phosphatase (*ALP*; Hs00758162_m1), osteocalcin (*OC*; Hs00609452_g1), collagen type I (*Coll I*; Hs00164004), runt-related transcription factor 2 (*Runx2*; Hs00231692_m1), and glyceraldehyde 3-phosphate dehydrogenase (*GAPDH*; Hs99999905). Relative expression for each gene was evaluated using the 2-$\Delta\Delta C_t$ method.[36] The C_t values of target genes were normalized by the C_t of the TaqMan human housekeeping gene *GAPDH* to obtain the ΔC_t values. The C_t of hUCMSCs cultured on TCPS in the control media for 1 day served as the calibrator.[23,26,36]

Mineral synthesis via hUCMSCs

Mineral synthesis via hUCMSCs released from the microbeads and proliferated on CPC-grafted-RGD was measured. The constructs were cultured in osteogenic media for 4, 7, 14, and 21 days ($n = 5$). Alizarin red S (ARS) staining was then performed to visualize mineralization.[37] The CPC-grafted-RGD samples seeded with hUCMSC microbeads were washed with PBS, fixed with 10% formaldehyde, and stained with ARS (Millipore, Billerica, MA) for 5 min, which stained calcium-rich deposits made by the cells into a red color. An osteogenesis assay kit (Millipore) was used to extract the stained minerals and measure the Alizarin red concentration at OD405, following the manufacturer's instructions. CPC samples without hUCMSCs were included as control. The control samples were cultured in the same manner for the same periods of time as the samples with cells. The value from the corresponding control sample was subtracted from the sample seeded with hUCMSCs to obtain the net mineral synthesis by the cells. Time periods of up to 21 days were selected because in previous studies a great increase in calcium content during *in vitro* cell cultures was found between 12 and 21 days.[37]

Measurement of physical and mechanical properties

The pH of the CPC paste was measured for CPC control, CPC-mixed-Fn, CPC-mixed-RGD, and CPC-grafted-RGD. A pH meter (Excel XL25; Fisher Scientific) was used, and the electrode was calibrated with three standard buffer solutions at pH of 4, 7, and 10, respectively. To avoid CPC setting and enable pH measurement, the pH of the cement paste was measured in a slurry with a water:CPC paste mass ratio of 9:1, following a previous study.[38] The pH was measured every 30 min for 48 h. Three slurries were tested for each CPC ($n = 3$).

Cement setting time was measured using a method described in a previous study.[30] CPC paste was mixed at a powder:liquid ratio of 2:1, filled into a mold of $3 \times 4 \times 25$ mm, and placed in a humidor at 37°C. At one-minute intervals, the specimen was scrubbed gently with figures until the powder component did not come off, indicating that the setting reaction had occurred sufficiently to hold the specimen together. The time measured from the powder–liquid mixing to this point was used as the setting time ($n = 5$).[30]

To measure porosity, CPC specimens of $3 \times 4 \times 25$ mm were incubated at 37°C in distilled water for 24 days, and then dried in a vacuum oven at 60°C for 24 h. CPC density, d, was measured using the specimen weight divided by volume, following a previous study.[39] Since all the CPC specimens contained CN, the specimen was a composite of hydroxyapatite (HA) and CN. Hence, the pore volume

fraction was estimated as $p=(d_{HA+CN}-d)/d_{HA+CN}$, where d_{HA+CN} is the theoretical density of the fully dense HA-CN composite.[39] The density of fully dense HA is $d_{HA}=3.14\,g/cm^3$.[39] CPC contained 15% CN in the liquid, and $d_{HA+CN}=2.82\,g/cm^3$, as obtained in a previous study.[39] Therefore, the measured density d leads to the calculation of the porosity p ($n=5$). In addition, specimens of CPC control, CPC-mixed-Fn, CPC-mixed-RGD, and CPC-grafted-RGD were sputter-coated with gold and examined in a scanning electron microscope (SEM; FEI Quanta 200, Hillsboro, OR). Both external surfaces and interior cross sections of CPC specimens were examined.

For mechanical testing, CPC bars of $3\times4\times25$ mm were fabricated. A three-point flexural test was used to fracture the specimens on a Universal Testing Machine (MTS, Eden Prairie, MN) using a span of 20 mm at a crosshead speed of 1 mm/min. Flexural strength $S=3FL/(2bh^2)$, where F is the maximum load on the load–displacement (F–d) curve, L is span, b is specimen width, and h is thickness. Elastic modulus $E=(F/d)\times(L^3/[4bh^3])$. Work-of-fracture (toughness) was the area under the F–d curve divided by the specimen's cross-sectional area.[30]

One-way and two-way analysis of variance were performed to detect significant effects of the variables. Tukey's

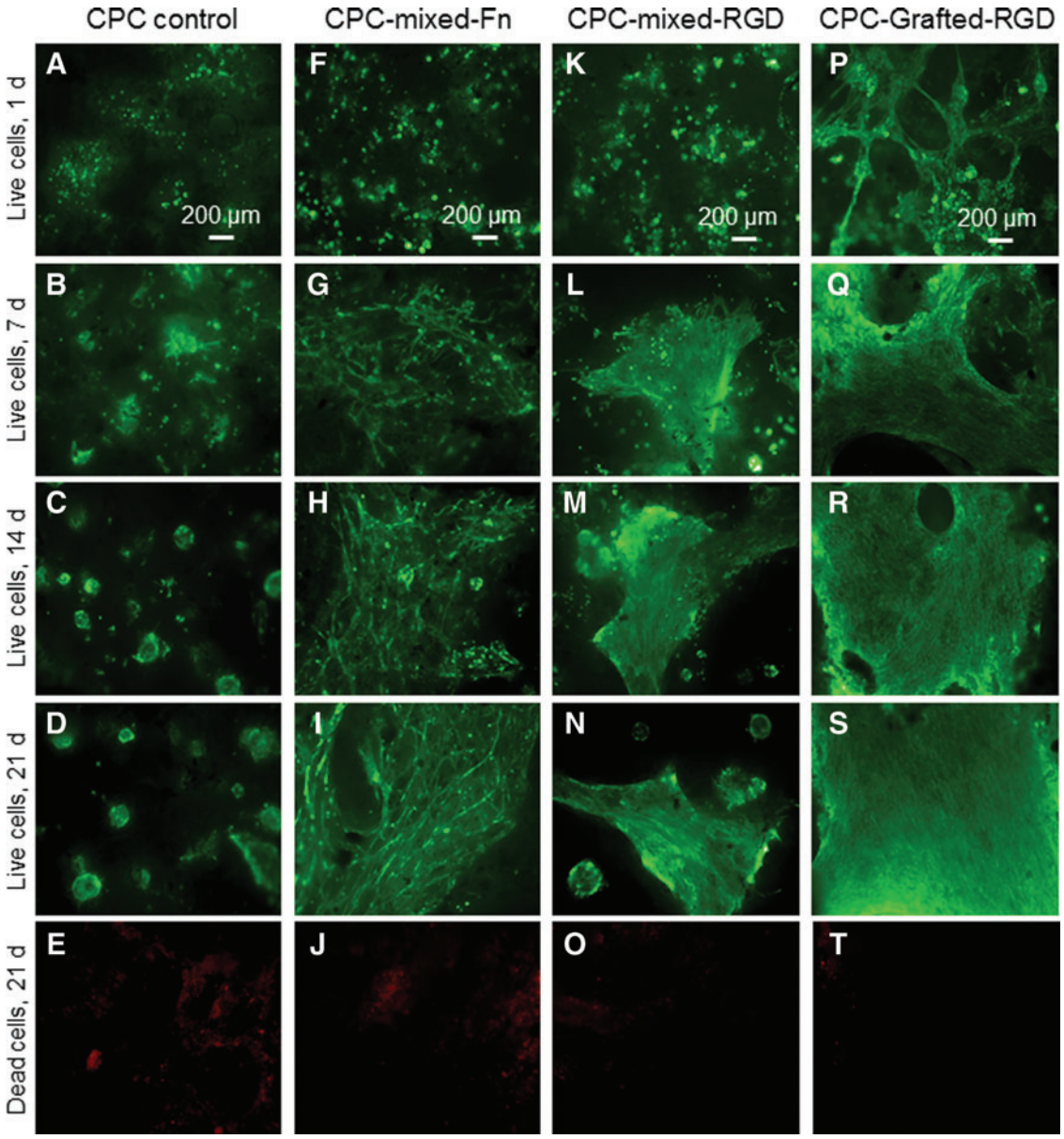

FIG. 2. Live/dead staining photos of hUCMSC-encapsulating microbeads in the CPC surface **(A–T)**. The scaffold type is listed on the top of each column: CPC control, CPC-mixed-Fn, CPC-mixed-Arg-Gly-Asp (RGD), and CPC-grafted-RGD. The culture times are listed on the left side for each row: 1, 7, 14, and 21 days. The first four rows show live cells (stained green). The last row shows dead cells (red). There were numerous live cells, and few dead cells. Incorporation of Fn and RGD into CPC increased cell attachment and proliferation. CPC control had the least cells. CPC-grafted-RGD appeared to have the most cells. Color images available online at www.liebertonline.com/tea

multiple comparison tests were used to compare the data at a p-value of 0.95.

Results

Figure 1A–D shows the schematic of alginate-fibrin microbead partially embedded in CPC, illustrating microbead degradation over time, and cell release onto CPC. Optical photos of the microbeads are shown in Figure 1E and F, at 1 and 14 days, respectively. Microbeads degraded over time and cells were released and attached to CPC at 7 days. Cells inside the microbeads appeared as rounded dots in Figure 1E, while in Figure 1F the released cells had a spreading and elongated morphology.

The live/dead staining photos are shown in Figure 2. CPC control had limited amount of live cells. The released cells did not attach well to CPC, and some cells likely were lost during media change. CPC-grafted-RGD had the best cell attachment and the fastest proliferation. There were few dead cells (stained red), shown in Figure 2 (last row) for 21 days as an example.

Figure 3A and B plots the percentage of live cells and live cell density, for the hUCMSCs released from the microbeads and attached on CPC. In Figure 3A, CPC-mixed-Fn and CPC-mixed-RGD had similar percentages of live cells ($p > 0.1$). CPC-grafted-RGD had the highest percentage of live cells ($p < 0.05$). In Figure 3B, the number of live cells per CPC surface area (mm^2) increased with increasing time due to proliferation. At 21 days, compared with CPC control, the live cell density was increased ninefold when the RGD was grafted with CPC.

The RT-PCR results of CPC-grafted-RGD are plotted in Figure 4A–D for *ALP*, *OC*, *Coll I*, and *Runx2* gene expression. All four markers reached much higher levels than day 1, indicating successful osteogenic differentiation of the hUCMSCs released from the microbeads and attached to the CPC-grafted-RGD scaffold.

Figure 5 shows the mineralization results for hUCMSCs released from the microbeads and attached to CPC-grafted-RGD. Disks without cells were immersed as control for the same time periods, with an example in Figure 5A at 21 days. In Figure 5B, the disk with cells at 7 days stained red. However, when the culture time was increased to 14 and 21 days (Fig. 5C and D, respectively), an additional red substance accumulated on the disks. The red staining became thicker and denser over time, and the layer of new mineral matrix synthesized by the cells covered the entire disk at 21 days (Figure 5D). The thick matrix mineralization by the cells covered not only the top surface, but also the peripheral areas of the scaffold at 21 days. The mineral concentration via an osteogenesis assay is plotted in Figure 5E. The mineral synthesis by the hUCMSCs released from microbeads and attached to CPC-grafted-RGD was minimal at 4 and 7 days, but greatly increased at 14 and 21 days ($p < 0.05$).

Figure 6 shows the physical properties of CPC. In Figure 6A, CPC-grafted-RGD had significantly higher pH values than the other materials ($p < 0.05$). In Figure 6B, all the CPCs had similar setting times of around 7 min ($p > 0.1$). In Figure 6C and D, the CPC density and porosity were also not affected by the incorporation of Fn and RGD ($p > 0.1$), with a pore volume fraction of ~52%. Representative SEM images of CPC-grafted-RGD specimen surfaces are shown in Figure 6E and F, at low and high magnifications, respectively. Arrows in Figure 6E indicate pores of sizes of a few tens of microns. Higher magnification of CPC in Figure 6F revealed numerous small pores of about one micron to several microns. SEM examination of other CPCs showed that all CPCs had similar porous features in the external surfaces and the interior cross sections.

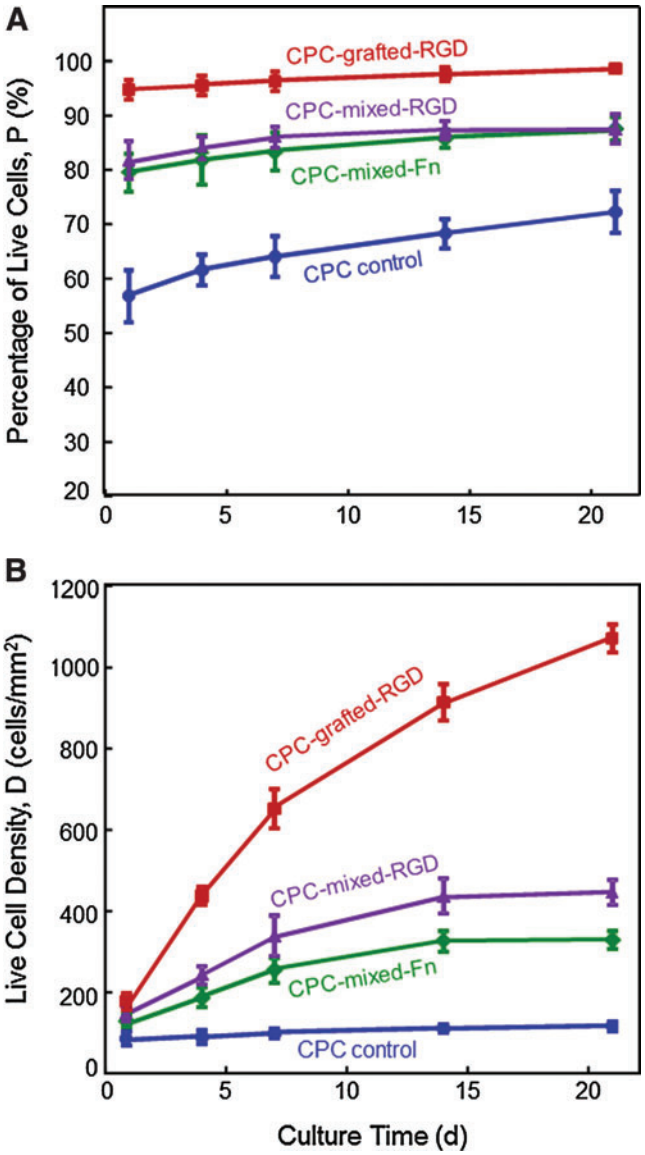

FIG. 3. Quantitative cell viability of hUCMSCs released from the microbeads and attached to CPC. **(A)** Percentage of live cells, and **(B)** live cell density. CPC-grafted-RGD had the highest percentages of live cells. CPC-grafted-RGD had the most live cell density per mm^2. Each value is the mean of five measurements, with the error bar showing one standard deviation (mean ± SD; $n = 5$). Color images available online at www.liebertonline.com/tea

Figure 7A–C plots the flexural strength, elastic modulus, and work-of-fracture (toughness) of CPC composites. Mixing Fn or RGD into CPC did not decrease the mechanical properties of CPC, compared with that without bioactive agents. CPC grafted with RGD had higher mechanical properties than the other three materials ($p < 0.05$).

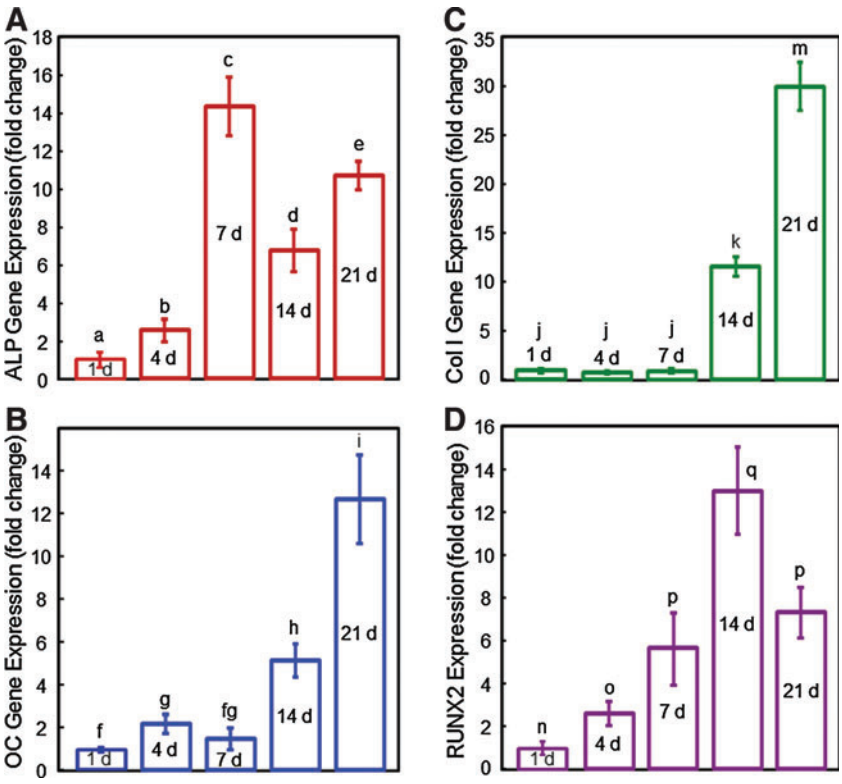

FIG. 4. Osteogenic differentiation of hUCMSC-encapsulating microbeads in CPC-grafted-RGD surface. **(A)** Alkaline phosphatase, **(B)** osteocalcin, **(C)** collagen type I, and **(D)** Runx2 gene expression, measured by real-time reverse transcription–polymerase chain reaction. All four markers reached much higher levels than day 1, indicating successful osteogenic differentiation of the hUCMSCs released from the microbeads and attached to the CPC-grafted-RGD scaffold. Each value is mean ± SD; $n = 5$. Color images available online at www.liebertonline.com/tea

Discussion

This study showed that (1) hUCMSC-encapsulating alginate-fibrin microbeads in the surface of biofunctionalized CPC released the cells that attached to CPC and differentiated down the osteogenic lineage and (2) incorporating biofunctional molecules of RGD and Fn greatly improved the cell function on CPC. The novel CPC-grafted-RGD construct had the highest number of live cells, without comprising the CPC mechanical properties. A literature search indicated that microbeads of several hundred micrometers in size that could quickly degrade and release the cells in a few days were not available. Several studies reported larger fibrin beads of about 3 mm in diameter for cell encapsulation.[40,41] These beads are not suitable for injection because they are larger than the needle sizes; for example, needles with gauge sizes of 10, 12, 14, 16, and 21 have inner diameters of 2.69, 2.16, 1.60, 1.19, and 0.51 mm, respectively. One study reported fibrin microbeads of 50–300 μm in diameter prefabricated in hot oil and then seeded with cells on the surfaces,[42] without cell encapsulation inside the microbeads. Other studies developed alginate beads of 3.6- and 2.2-mm diameters for cell encapsulation; these beads were not fast degradable and the previous studies did not report cell release from these beads.[24] Another study fabricated RGD-modified alginate microbeads of 1 mm in diameter, and the authors did not report bead degradation or cell release.[43] In our previous study,[23] alginate microbeads of 207 μm were developed to encapsulate cells, but the microbeads were not degradable and no cell release was obtained. Therefore, cell-encapsulating microbeads that could quickly degrade and release the cells are unique.

The fast-degradable microbeads of the present study were fabricated by adding a small amount of fibrin into the oxidized alginate. Oxidized alginate without fibrin was not fast degradable. Fibrin is a natural fibrous protein involved in the clotting of blood, via polymerization from fibrinogen and thrombin into a mesh structure that can form a hemostatic clot over a wound site. Previous studies developed fibrin as a tissue substitute for bone, cartilage, and other tissue regenerations.[44] The alginate-fibrin microbeads of the present study could be mixed with a CPC paste or a polymer paste for injection delivery in minimally invasive procedures. The paste could also be shaped to achieve contours for esthetics in dental and craniofacial applications. Then, the paste would harden to form a scaffold to support stresses and guide tissue regeneration. The scaffold could provide mechanical support and a porous volume for cell attachment. Once the scaffold is set, it is beneficial for the microbeads to quickly degrade and release the cells inside the scaffold, while the microbead degradation creates macropores. Without cell release, the cells inside a hydrogel had contact inhibition; therefore, the cell proliferation became arrested.[45] As a result, cells encapsulated in the microbeads had shapes as rounded dots (Fig. 1E) with no proliferation. In contrast, cells released from the microbeads could attach to the scaffold and proliferate, as shown in Figure 1F and Figure 2. In preliminary study, alginate microbeads showed no degradation and negligible cell release at 21 days. The oxidized alginate microbeads showed slight degradation and some cell release at 21 days. In dramatic contrast, the oxidized alginate-fibrin microbeads showed significant degradation and cell release at 7 days. Therefore, adding fibrin to alginate resulted in fast cell release from the microbeads, likely due to

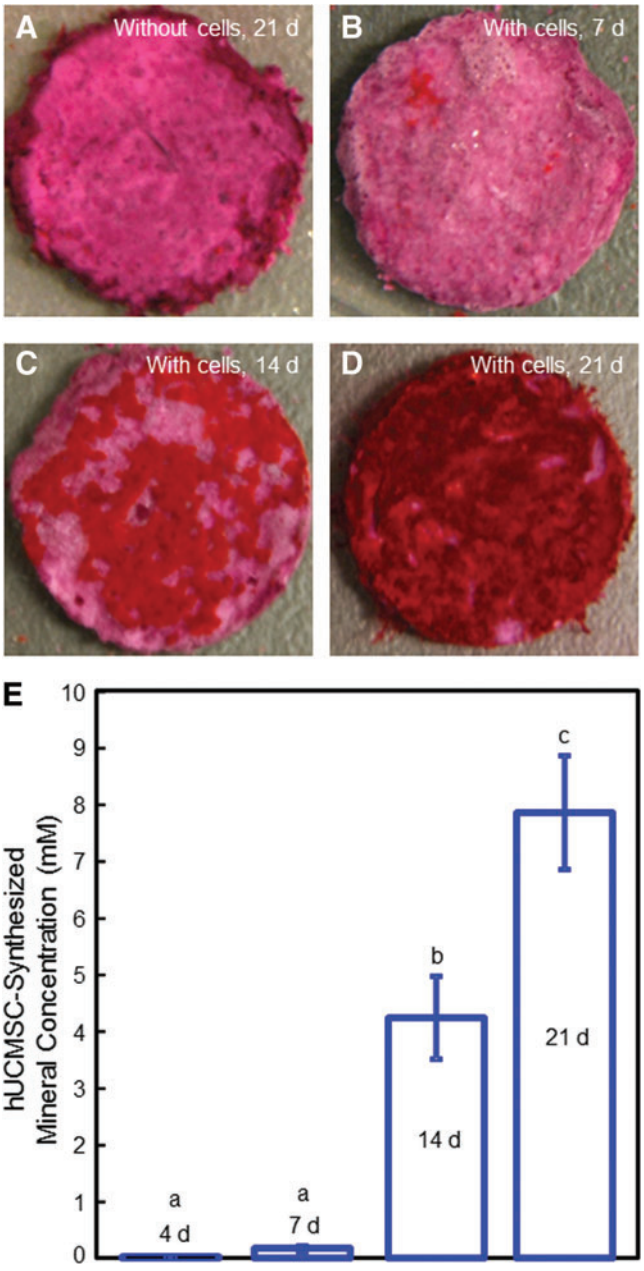

FIG. 5. Bone mineral synthesis by hUCMSCs released from the microbeads and attached to the CPC-grafted-RGD disks. **(A)** Disks without cells were immersed as control. **(B)** Disk with cells at 7 days. **(C)** Disk with cells at 14 days. **(D)** Disk with cells at 21 days. The red staining became much thicker and denser over time, and the layer of new mineral matrix synthesized by the cells covered the entire disk at 21 days. **(E)** Cell-synthesized mineral concentration was measured by the osteogenesis assay. Each value is mean ± SD; $n = 5$. Values with dissimilar letters are significantly different ($p < 0.05$). Color images available online at www.liebertonline.com/tea

two reasons. First, because fibrin has a porous fibrous structure, adding fibrin appeared to loosen the alginate structure, resulting in mechanically weaker microbeads that were readily degradable.[26] Second, fibrin was known to enhance cell attachment and proliferation.[44] Microscopic examination suggested that the cells inside the alginate-fibrin microbeads were spreading and proliferating. This would increase the internal pressure in the microbeads, thus accelerating the breakdown of microbeads. It should be noted that the present study embedded the microbeads into the CPC paste surface. The microbeads degraded and released the cells. The cells attached to the flat CPC surface, which enabled live/dead staining and yielded well-focused images. In clinical applications, the microbeads would be randomly mixed with the CPC paste, and the cells would be released within the CPC scaffold. Therefore, the CPC scaffold needs to have highly interconnected macroporosity to provide fluid circulation. The CPC scaffolds had a porosity of 52% (Fig. 6D). This was the intrinsic porosity of CPC, due to powder-liquid mixing that could trap air bubbles, and the water in the paste creating porosity in the set CPC. Further study should incorporate porogens and resorbable fibers into CPC to create interconnected macropores with stem cell release within the CPC scaffold.

When the hUCMSCs are released from the microbeads, it is desirable for them to attach to CPC and proliferate. However, preliminary study showed that the released cell attachment to CPC was not robust, which is consistent with previous studies showing poor human stem cell attachment to CPC.[46,47] Therefore, there was a need to biofunctionalize CPC. Both Fn and RGD are known to be effective in improving cell attachment. These biofunctional molecules have been used in polymeric and pre-formed calcium phosphate scaffolds.[2,4,31–37] However, to date there has been no report on incorporating Fn or RGD into injectable CPC paste.

Since RGD peptides (R: arginine; G: glycine; D: aspartic acid) were found to promote cell adhesion in 1984,[48] numerous materials have been RGD functionalized.[2,4,33–42,49–52] RGD is the principal integrin-binding domain present in extracellular matrix proteins, including Fn, vitronectin, fibrinogen, osteopontin, and bone sialoprotein. One advantage of RGD is that its functionality is usually maintained in biomaterial processing and sterilization steps without protein denaturation. Another advantage is that the synthesis of RGD is relatively simple and inexpensive. The third advantage is that RGD can be readily coupled to biomaterial surfaces in controlled densities and orientations to enhance and guide cell function. *In vitro* studies demonstrated that RGD-functionalized polymers improved cell attachment, growth, and biological function.[37,49–52] *In vivo* investigations showed the capability of RGD-modified polymers for enhancing bone healing.[53,54] In addition, studies reported the Fn enrichment of scaffolds, including HA, showing better proliferation of osteoblasts, which were higher in the group enriched with the highest concentration of Fn.[31,32,55,56]

In the present study, mixing 0.25 mg of Fn or RGD in each CPC disk with about 0.9 g of CPC paste resulted an Fn or RGD concentration of ~0.03% by mass. The greatest increase in live cell density was achieved when the RGD was grafted to CN, and the CN liquid was then mixed with CPC. In previous studies, physical adsorption of RGD on the surface of HA scaffolds was a common method.[57,58] In comparison, chemically bonding the RGD with the scaffold showed much better anti-washout capability.[4,59,60] In fabricating the CPC-mixed-RGD scaffold, the RGD was first mixed with the CN liquid. The CN-RGD liquid was then mixed with the CPC powder, and the paste was hardened. This process provided mechanical interlocking of RGD molecules in the CPC. While

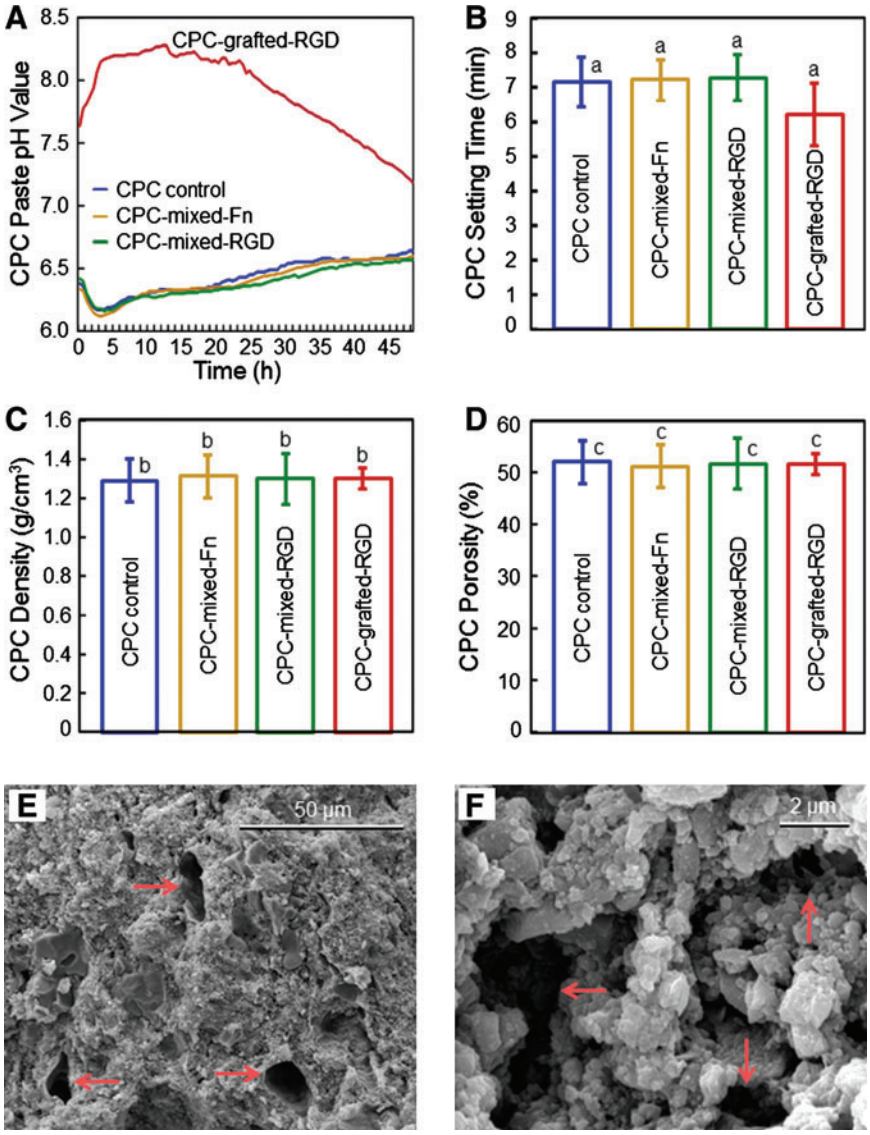

FIG. 6. Physical properties of CPC. **(A)** pH of CPC paste slurry. The results shown are the mean of three measurements ($n=3$). The error bars were omitted for clarity, and were around 2% to 5% of the mean values. **(B)** CPC setting time. **(C)** CPC density. **(D)** CPC pore volume fraction. For **B–D**, each value is mean ± SD; $n=5$. In each plot, values with the same letters are not significantly different ($p>0.1$). **(E, F)** Representative SEM images of CPC-grafted-RGD specimen surfaces. Arrows indicate the pores. All four CPCs had similar porous features in both the external surfaces and the interior cross sections. SEM, scanning electron microscope. Color images available online at www.liebertonline.com/tea

some RGD in the set CPC may still leach out during culture media change, this method is expected to retain RGD better than the method of simply coating RGD onto the external surface of a pre-fabricated implant. Further, for CPC-grafted-RGD, by bonding and immobilizing the RGD-sequence-containing peptides with CN that was then mixed with CPC, the loss of RGD was minimized. This was likely responsible for the better cell attachment and higher live cell density on the CPC-grafted-RGD scaffold, compared with CPC-mixed-RGD.

The hUCMSCs that migrated out of the microbeads and attached to CPC-grafted-RGD were differentiated down the osteogenic lineage. RT-PCR showed that the *ALP* peaked at 7 days, while *OC* peaked at a later time of 21 days. *ALP* is an enzyme expressed by MSCs during osteogenesis and is a well-defined marker for their differentiation.[11,12,36,61] At the early stage of osteogenic differentiation, the *ALP* is first upregulated.[36] Then, as the cascade of events for differentiation continues, other markers—such as *Runx2*, *OC*, and *Coll I*—become upregulated, while *ALP* decreased.[36] The observation that a bone marker expression increased with time, reached a peak, and then decreased with time is consistent with previous studies. For example, one study showed that the *ALP* peaked at 8 days and then decreased at 16 days.[61] Another study demonstrated that the *ALP* peaked at 4 days, and then decreased at 8 days.[36] In the present study, the *ALP* peaked at 7 days and then decreased; *Runx2* peaked at 14 days and then decreased. The sequence that certain bone markers peaked earlier than other markers is also consistent with previous studies. For example, a study reported that the *OC* peaked at 8 days, later than *ALP* that peaked at 4 days, indicating that *OC* was upregulated at a later stage than *ALP*.[36] This sequence agrees with the present study, where the *ALP* peak was earlier than the *OC* peak. It should be noted that while there exists a sequence for the osteogenic differentiation stages, the exact peaking time appeared to vary with the construct culture conditions. In the present study, it may have taken a longer time for the hUCMSCs to express peaking values for the bone markers than previous studies. This is because the hUCMSCs were encapsulated in

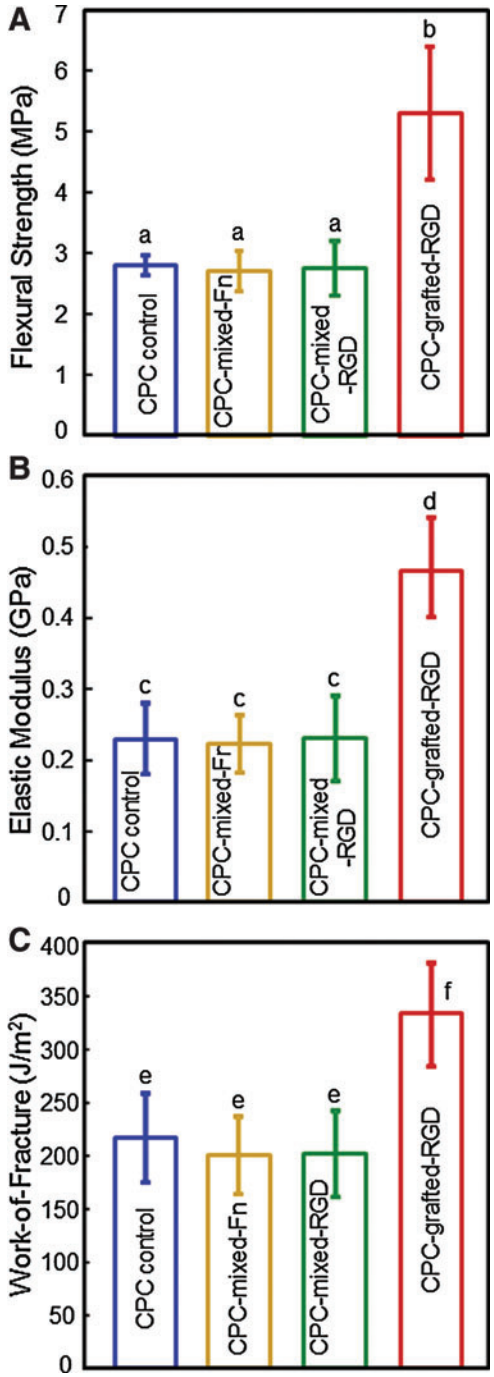

FIG. 7. Mechanical properties of biofunctionalized CPC containing various biofunctional molecules. **(A)** Flexural strength, **(B)** elastic modulus, and **(C)** work-of-fracture (toughness). Each value is mean ± SD; $n = 5$. Values with dissimilar letters are significantly different ($p < 0.05$). Color images available online at www.liebertonline.com/tea

microbeads, and it took time for the microbeads to degrade and for the cells to attach to the CPC-grafted-RGD scaffold. In addition, ARS staining revealed a thick layer of mineral made by cells at 14 and 21 days that covered the CPC-grafted-RGD disks. Hence, the hUCMSC-CPC-grafted-RGD construct is promising for bone tissue engineering. Umbilical cords are inexhaustible and can be collected at a low cost. hUCMSCs can be harvested without the invasive procedure needed for bone marrow MSCs, and are promising for regenerative medicine.[13,27,28,62] Previous studies showed that hUCMSCs had excellent potential for bone engineering.[24,28,63] The present study confirmed the potential of hUCMSCs, and showed that the hUCMSCs released from fast-degradable microbeads in CPC had excellent proliferation with osteogenic differentiation and mineral synthesis.

RGD grafting could affect the mechanical properties of the biomaterial. In a previous study, RGD, YIGSR (Tyr-Ile-Gly-Ser-Arg), and IKVAV (Ile-Lys-Val-Ala-Val) were conjugated with cross-linked poly(ethylene glycol) hydrogels.[64] Grafting with ligands significantly affected the properties of the hydrogels.[64] In another report, rheological analysis of RGD-conjugated CN-pluronic hydrogels showed that the RGD-conjugated hydrogels had higher storage modulus of about 100 kPa.[65] This was a substantial increase, as the storage moduli of hydrogels without RGD were about 10 kPa.[65,66] These previous results are consistent with the present study that showed that RGD grafting increased the mechanical properties of CPC. There has been no report on adding RGD to CPC, and the reason for the mechanical property increase needs further investigation. It was noticed that the RGD-functionalized CN solution was significantly stickier than the other CN solutions in the present study. The stickier RGD-functionalized CN may have acted as a good gelling agent to bind the CPC components together to form a strong scaffold. Figure 6A showed that the CPC paste using RGD-grafted CN had a higher pH than the other CPC pastes. Further study is needed to understand why RGD grafting increases the pH of CPC paste and the mechanical properties of CPC, and whether pH and mechanical properties are related. For CPC-grafted-RGD, the RGD was covalently bonded to CN, which was then mixed with CPC. Previous studies showed that the incorporation of CN shortened the setting time of CPC, avoided CPC paste washout, and increased the CPC strength.[30] The present study showed that another function of CN was that it served as a vehicle to incorporate RGD into CPC. Therefore, RGD grafting with CN-CPC scaffold not only enhanced cell attachment and proliferation, but also improved the scaffold mechanical properties. Further studies should investigate how to translate these improvements into bone regeneration in an animal model.

Conclusions

hUCMSC-encapsulating alginate-fibrin microbeads were embedded on the surface of novel biofunctionalized CPC, and the cell release from microbeads and attachment to CPC were investigated. Biofunctionalized CPCs were developed that greatly enhanced the attachment of the released hUCMSCs. The new CPC-grafted-RGD showed the fastest cell proliferation and highest live cell density, which was nearly an order of magnitude higher than that of CPC control without biofunctional molecules. Bone marker expression of hUCMSCs on CPC-grafted-RGD increased by 10 to 30 fold at 7–21 days, compared with control at day 1. The released cells on CPC-grafted-RGD synthesized bone minerals, with a new mineral layer accumulating on the scaffold. hUCMSC mineralization increased by two orders of magnitude from 7 to 21 days. This study showed the

promise for alginate-fibrin microbeads in CPC to fast degrade and release the cells, and for CPC-grafted-RGD to enhance cell function and bone regeneration. For potential applications, the microbeads could be mixed with the CPC paste and the paste can be injected or placed into a bone defect. After setting, the microbeads could quickly degrade and release the cells throughout CPC scaffold, while creating macropores to enhance cell migration and tissue ingrowth. Future study needs to investigate the *in vivo* bone regeneration via the construct of cell–microbeads and biofunctionalized CPC in an animal model.

Acknowledgments

This study was supported by NIH grants R01DE17974 and R01DE14190 (H.X.), Maryland Stem Cell Fund (H.X.), and the University of Maryland School of Dentistry.

Disclosure Statement

No competing financial interests exist.

References

1. Atala, A. Engineering organs. Curr Opin Biotechnol **20,** 575, 2009.
2. Hill, E., Boontheekul, T., and Mooney, D.J. Designing scaffolds to enhance transplanted myoblast survival and migration. Tissue Eng **12,** 1295, 2006.
3. Mao, J.J., Giannobile, W.V., Helms, J.A., Hollister, S.J., Krebsbach, P.H., Longaker, M.T., and Shi, S. Craniofacial tissue engineering by stem cells. J Dent Res **85,** 966, 2006.
4. Salinas, C.N., and Anseth, K.S. The influence of the RGD peptide motif and its contextual presentation in PEG gels on human mesenchymal stem cell viability. J Tissue Eng Reg Med **2,** 296, 2008.
5. Kretlow, J.D., Young, S., Klouda, L., Wong, M., and Mikos, A.G. Injectable biomaterials for regenerating complex craniofacial tissues. Adv Mater **21,** 3368, 2009.
6. Gomes, ME., Mikos, A.G., and Reis, R.L. Injectable Polymeric Scaffolds for Bone Tissue Engineering. In: Reis, R.L., San Roman, J., eds. Biodegradable Systems in Tissue Engineering and Regenerative Medicine. Boca Raton, FL: CRC Press, 2004, pp. 29–38.
7. Mikos, A.G., Herring, S.W., Ochareon, P., Elisseeff, J., Lu, H.H., Kandel, R., Schoen, F.J., Toner, M., Mooney, D., Atala, A., Van Dyke, M.E., Kaplan, D., and Vunjak-Novakovic, G. Engineering complex tissues. Tissue Eng **12,** 3307, 2006.
8. Johnson, P.C., Mikos, A.G., Fisher, J.P., and Jansen, J.A. Strategic directions in tissue engineering. Tissue Eng **13,** 2827, 2007.
9. Praemer, A., Furner, S., and Rice, D.P. Musculoskeletal conditions in the United States. Rosemont, IL: Amer Acad Orthop Surg, 1999.
10. Jansen, J.A., Vehof, J.W.M., Ruhe, P.Q., Kroeze-Deutman, H., Kuboki, Y., Takita, H., Hedberg, E.L., and Mikos, A.G. Growth factor-loaded scaffolds for bone engineering. J Controlled Release **101,** 127, 2005.
11. Benoit, D.S.W., Nuttelman, C.R., Collins, S.D., and Anseth, K.S. Synthesis and characterization of a fluvastatin-releasing hydrogel delivery system to modulate hMSC differentiation and function for bone regeneration. Biomaterials **27,** 6102, 2006.
12. Reilly, G.C., Radin, S., Chen, A.T., and Ducheyne, P. Differential alkaline phosphatase responses of rat and human bone marrow derived mesenchymal stem cells to 45S5 bioactive glass. Biomaterials **28,** 4091, 2007.
13. Sarugaser, R., Lickorish, D., Baksh, D., Hosseini, M.M., and Davies, J.E. Human umbilical cord perivascular (HUCPV) cells: A source of mesenchymal progenitors. Stem Cells **23,** 220, 2005.
14. Drury, J.L., and Mooney, D.J. Review. Hydrogels for tissue engineering: scaffold design variables and applications. Biomaterials **24,** 4337, 2003.
15. Drury, J.L., Dennis, R.G., and Mooney, D.J. The tensile properties of alginate hydrogels. Biomaterials **25,** 3187, 2004.
16. Brown, W.E., and Chow, L.C. A new calcium phosphate water setting cement. In: Brown, P.W., ed. Cements Research Progress. Westerville, OH: American Ceramic Society, 1986, pp. 352–379.
17. Bohner, M., and Baroud, G. Injectability of calcium phosphate pastes. Biomaterials **26,** 1553, 2005.
18. Link, D.P., van den Dolder, J., van den Beucken, J.J., Wolke, J.G., Mikos, A.G., and Jansen, J.A. Bone response and mechanical strength of rabbit femoral defects filled with injectable CaP cements containing TGF-b1 loaded gelatin microspheres. Biomaterials **29,** 675, 2008.
19. Friedman, C.D., Costantino, P.D., Takagi, S., and Chow, L.C. BoneSource hydroxyapatite cement: a novel biomaterial for craniofacial skeletal tissue engineering and reconstruction. J Biomed Mater Res **43B,** 428, 1998.
20. Xu, H.H.K., Chow, L.C., Takagi, S., and Eichmiller, F.C. Self-hardening calcium phosphate materials with high resistance to fracture, controlled strength histories and tailored macropore formation rates. U.S. Patent No. 6, 955, 716, 2005.
21. Zhao, L., Burguera, E.F., Xu, H.H.K., Amin, N., Ryou, H., and Arola, D.D. Fatigue and human umbilical cord stem cell seeding characteristics of calcium phosphate-chitosan-biodegradable fiber scaffolds. Biomaterials **31,** 840, 2010.
22. Zuo, Y., Yang, F., Wolke, J.G., Li, Y., and Jansen, J.A. Incorporation of biodegradable electrospun fibers into calcium phosphate cement for bone regeneration. Acta Biomater **6,** 1238, 2010.
23. Zhao, L., Weir, M.D., and Xu, H.H.K. An injectable calcium phosphate - alginate hydrogel - umbilical cord mesenchymal stem cell paste for bone tissue engineering. Biomaterials **31,** 6502, 2010.
24. Xu, H.H.K., Zhao, L., and Weir, M.D. Stem cell-calcium phosphate constructs for bone engineering. J Dent Res **89,** 1482, 2010.
25. Bouhadir, K.H., Lee, K.Y., Alsberg, E., Damm, K.L., Anderson, K.W., and Mooney, D.J. Degradation of partially oxidized alginate and its potential application for tissue engineering. Biotech Progress **17,** 945, 2001.
26. Zhou, H., and Xu, H.H.K. The fast release of stem cells from alginate-fibrin microbeads in injectable scaffolds for bone tissue engineering. Biomaterials **32,** 7503, 2011.
27. Wang, H.S., Hung, .SC., and Peng, S.T. Mesenchymal stem cells in the Wharton's jelly of the human umbilical cord. Stem Cells **22,** 1330, 2004.
28. Baksh, D., Yao, R., and Tuan, R.S. Comparison of proliferative and multilineage differentiation potential of human mesenchymal stem cells derived from umbilical cord and bone marrow. Stem Cells **25,** 1384, 2007.
29. Muzzarelli, R.A.A., Biagini, G., Bellardini, M., Simonelli, L., Castaldini, C., and Fraatto, G. Osteoconduction exerted by methylpyrolidinone chitosan in dental surgery. Biomaterials **14,** 39, 1993.

30. Xu, H.H.K., Takagi, S., Quinn, J.B., and Chow, L.C. Fast-setting and anti-washout calcium phosphate scaffolds with high strength and controlled macropore formation rates. J Biomed Mater Res A **68,** 725, 2004.
31. Schönmeyr, B.H., Wong, A.K., Li, S., Gewalli, F., Cordiero, P.G., and Mehrara, B.J. Treatment of hydroxyapatite scaffolds with fibronectin and fetal calf serum increases osteoblast adhesion and proliferation *in vitro*. Plast Reconstr Surg **121,** 751, 2008.
32. Place, E.S., Evans, N.D., and Stevens, M.M. Complexity in biomaterials for tissue engineering. Nat Mater **8,** 457, 2009.
33. Barker, T.H. The role of ECM proteins and protein fragments in guiding cell behavior in regenerative medicine. Biomaterials **32,** 4211, 2011.
34. Hsiong, S.X., Boontheekul, T., Huebsch, N., and Mooney, D.J. Cyclic arginine-glycine-aspartate peptides enhance three-dimensional stem cell osteogenic differentiation. Tissue Eng Part A **15,** 263, 2009
35. Grellier, M., Granja, P.L., Fricain, J.C., Bidarra, S.J., Renard, M., Bareille, R., Bourget, C., Amédée, J., and Barbosa, M.A. The effect of the co-immobilization of human osteoprogenitors and endothelial cells within alginate microspheres on mineralization in a bone defect. Biomaterials **30,** 3271, 2009.
36. Kim, K., Dean, D., Mikos, A.G., and Fisher, J.P. Effect of initial cell seeding density on early osteogenic signal expression of rat bone marrow stromal cells cultured on cross-linked poly(propylene fumarate) disks. Biomacromolecules **10,** 1810, 2009.
37. Wang, Y.H., Liu, Y., Maye, P., and Rowe, D.W. Examination of mineralized nodule formation in living osteoblastic cultures using fluorescent dyes. Biotechnol **22,** 1697, 2006.
38. Bohner, M., Van Landuyt, P., Merkle, H.P., and Lemaitre, J. Composition effects on the pH of a hydraulic calcium phosphate cement. J Mater Sci Mater Med **8,** 675, 1997.
39. Zhang, Y., Xu, H.H.K., Takagi, S., and Chow, L.C. *In-situ* hardening hydroxyapatite-based scaffold for bone repair. J Mater Sci: Mater in Med **17,** 437, 2006.
40. Perka, C., Arnold, U., Spitzer, R.S., and Lindenhayn, K. The use of fibrin beads for tissue engineering and subsequential transplantation. Tissue Eng **7,** 359, 2001.
41. Spitzer, R.S., Perka, C., Lindenhayn, K., and Zippel, H. Matrix engineering for osteogenic differentiation of rabbit periosteal cells using alpha-tricalcium phosphate particles in a three-dimensional fibrin culture. J Biomed Mater Res **59,** 690, 2002.
42. Gorodetsky, R., Levdansky, L., Gaberman, E., Gurevitch, O., Lubzens, E., and McBride, W.H. Fibrin microbeads (FMB) loaded with mesenchymal cells support their long term survival while sealed at room temperature. Tissue Eng Part C **17,** 745, 2011.
43. Evangelista, M.B., Hsiong, S.X., Fernandes, R., Sampaio, P., Kong, H.J., Barrias, C.C., Salema, R., Barbosa, M.A., Mooney, D.J., and Granja, P.L. Upregulation of bone cell differentiation through immobilization within a synthetic extracellular matrix. Biomaterials **28,** 3644, 2007.
44. Ahmed, T.A., Dare, E.V., and Hincke, M. Fibrin: a versatile scaffold for tissue engineering applications. Tissue Eng Part B **14,** 199, 2008.
45. Markusen, J.F., Mason, C., Hull, D.A., Town, M.A., Tabor, A.B., Clements, M., Boshoff, C.H., and Dunnill, P. Behavior of adult human mesenchymal stem cells entrapped in alginate-GRGDY beads. Tissue Eng **12,** 821, 2006.
46. Link, D.P., van den, D.J., Wolke, J.G., and Jansen, J.A. The cytocompatibility and early osteogenic characteristics of an injectable calcium phosphate cement. Tissue Eng **13,** 493, 2007.
47. Weir, M.D., and Xu, H.H.K. Culture human mesenchymal stem cells with calcium phosphate cement scaffolds for bone repair. J Biomed Mater Res **93B,** 93, 2010.
48. Pierschbacher, M.D., and Ruoslahti, E. Cell attachment activity of fibronectin can be duplicated by small synthetic fragments of the molecule. Nature **309,** 30, 1984.
49. Bellis, S.L. Advantages of RGD peptides for directing cell association with biomaterials. Biomaterials **32,** 4205, 2011.
50. Hers, U., Dahmen, C., and Kessler, H. RGD modified polymers: biomaterials for stimulated cell adhesion and beyond. Biomaterials **24,** 4385, 2003.
51. Chun, C., Lim, H.J., Hong, K.Y., Park, K.H., and Song, S.C. The use of injectable, thermosensitive poly(organophosphazene)-RGD conjugates for the enhancement of mesenchymal stem cell osteogenic differentiation. Biomaterials **30,** 6295, 2009.
52. Qu, Z., Yan, J., Li, B., Zhuang, J., and Huang, Y. Improving bone marrow stromal cell attachment on chitosan/hydroxyapatite scaffolds by an immobilized RGD peptide. Biomed Mater **5,** 065001,2010.
53. Park, J.W., Kurashima, K., Tustusmi, Y., An, C.H., Suh, J.Y., Doi, H., Nomura, N., Noda, K., and Hanawa, T. Bone healing of commercial oral implants with RGD immobilization through electrodeposited poly(ethylene glycol) in rabbit cancellous bone. Acta Biomater **7,** 3222, 2011.
54. Oest, M.E., Dupont, K.M., Kong, H.J., Mooney, D.J., and Guldberg, R.E. Quantitative assessment of scaffold and growth factor-mediated repair of critically sized bone defects. J Orthop Res **25,** 941, 2007.
55. Fernández, M.S., Arias, J.I., Martínez, M.J., Saenz, L., Neira-Carrillo, A., Yazdani-Pedram, M., and Arias, J.L. Evaluation of a multilayered chitosan-hydroxy-apatite porous composite enriched with fibronectin or an *in vitro*-generated bone-like extracellular matrix on proliferation and diferentiation of osteoblasts. J Tissue Eng Regen Med [Epub ahead of print]; DOI: 10.1002/term.455, 2011.
56. Sogo, Y., Ito, A., Matsuno, T., Oyane, A., Tamazawa, G., Satoh, T., Yamazaki, A., Uchimura, E., and Ohno, T. Fibronectin-calcium phosphate composite layer on hydroxyapatite to enhance adhesion, cell spread and osteogenic differentiation of human mesenchymal stem cells *in vitro*. Biomed Mater **2,** 116, 2007.
57. Sawyer, A.A., Hennessy, K.M., and Bellis, S.L. Regulation of mesenchymal stem cell attachment and spreading on hydroxyapatite by RGD peptides and adsorbed serum proteins. Biomaterials **26,** 1467, 2005.
58. Hennessy, K.M., Clem, W.C., Phipps, M.C., Sawyer, A.A,, Shaikh, F.M., and Bellis, S.L. The effect of RGD peptides on osseointegration of hydroxyapatite biomaterials. Biomaterials **29,** 3075, 2008.
59. Balasundaram, G., Sato, M., and Webster, T.J. Using hydroxyapatite nanoparticles and decreased crystallinity to promote osteoblast adhesion similar to functionalizing with RGD. Biomaterials **27,** 2798, 2006.
60. Durrieu, M.C., Pallu, S., Guillemot, F., Bareille, R., Amédée, J., Baquey, C.H., Labrugère, C., and Dard, M. Grafting RGD containing peptides onto hydroxyapatite to promote osteoblastic cells adhesion. J Mater Sci Mater Med **15,** 779, 2004.
61. Datta, N., Pham, Q.P., Sharma, U., Sikavitsas, V.I., Jansen, J.A., and Mikos, A.G. *In vitro* generated extracellular matrix

and fluid shear stress synergistically enhance 3D osteoblastic differentiation. Proc Natl Acad Sci USA **103,** 2488, 2006.
62. Can, A., and Karahuseyinoglu, S. Concise review: Human umbilical cord stroma with regard to the source of fetus-derived stem cells. Stem Cells **25,** 2886, 2007.
63. Diao, Y., Ma, Q., Cui, F., and Zhong, Y. Human umbilical cord mesenchymal stem cells: osteogenesis *in vivo* as seed cells for bone tissue engineering. J Biomed Mater Res A **91,** 123, 2009.
64. Zustiak, S.P., Durbal, R., and Leach, J.B. Influence of cell-adhesive peptide ligands on poly(ethylene glycol) hydrogel physical, mechanical and transport properties. Acta Biomater **6,** 3404, 2010.
65. Park, K.M., Joung, Y.K., Park, K.D., Lee, S.Y., and Lee, M.C. RGD-Conjugated Chitosan-Pluronic Hydrogels as a Cell Supported Scaffold for Articular Cartilage Regeneration. Macromolecular Res **16,** 517, 2008.
66. Jin, R., Hiemstra, C., Zhong, Z., and Feijen, J. Enzyme-mediated fast *in situ* formation of hydrogels from dextran-tyramine conjugates. Biomaterials **28,** 2791, 2007.

Address correspondence to:
Hockin H.K. Xu, Ph.D.
Director of Biomaterials & Tissue Engineering
Division Department of Endodontics, Prosthodontics and Operative Dentistry
University of Maryland School of Dentistry
Baltimore, MD 21201

E-mail: hxu@umaryland.edu

Hongzhi Zhou, D.D.S., Ph.D.
Department of Oral & Maxillofacial Surgery
School of Stomatology
Fourth Military Medical University
Xi'an, Shanxi 710032
China

E-mail: hz_zhou@yahoo.com

Received: November 8, 2011
Accepted: March 19, 2012
Online Publication Date: May 11, 2012